Topographical Functional Connectivity Pattern in the Perisylvian Language Networks

Hua-Dong Xiang[1], Hubert M. Fonteijn[1,2], David G. Norris[1,3] and Peter Hagoort[1,4]

[1]Donders Institute for Brain, Cognition and Behaviour, Radboud University Nijmegen, 6500 HB Nijmegen, The Netherlands, [2]Helmholtz Institute, Utrecht University, 3584 CS Utrecht, The Netherlands, [3]Erwin L. Hahn Institute for Magnetic Resonance Imaging, Arendahls Wiese 199, D-45141 Essen, Germany and [4]Max Planck Institute for Psycholinguistics, 6500 AH Nijmegen, The Netherlands

We performed a resting-state functional connectivity study to investigate directly the functional correlations within the perisylvian language networks by seeding from 3 subregions of Broca's complex (pars opercularis, pars triangularis, and pars orbitalis) and their right hemisphere homologues. A clear topographical functional connectivity pattern in the left middle frontal, parietal, and temporal areas was revealed for the 3 left seeds. This is the first demonstration that a functional connectivity topology can be observed in the perisylvian language networks. The results support the assumption of the functional division for phonology, syntax, and semantics of Broca's complex as proposed by the memory, unification, and control (MUC) model and indicated a topographical functional organization in the perisylvian language networks, which suggests a possible division of labor for phonological, syntactic, and semantic function in the left frontal, parietal, and temporal areas.

Keywords: Broca's complex, functional organization, pars opercularis (BA 44), pars orbitalis (BA 47), pars triangularis (BA 45)

Introduction

It has been suggested, based on Broca and Wernicke's classical clinical observations and many subsequent studies, that there is a neural loop that is involved in language processing (Ojemann 1991) located around the lateral sulcus (also known as the fissure of Sylvius). This is located in the dominant hemisphere (the left for most people), connected by the arcuate fasciculus. Broca's area lies at the rostral end of this loop; Wernicke's area is situated at the other end (in the superior posterior temporal lobe). The inferior parietal lobule, also known as "Geschwind's territory" (Catani et al. 2005), has also been implicated in language processing by recent neuroimaging studies. For example, several diffusion tensor imaging (DTI) studies showed that the inferior parietal lobule is connected by large bundles of nerve fibers to both Broca's area and Wernicke's area (Catani et al. 2005; Parker et al. 2005; Powell et al. 2006). Thus, besides the frontal and temporal language areas, the parietal lobe is now also thought to play an important role in the perisylvian language networks.

In the perisylvian language networks, Broca's area is the first area of the brain to have been associated with language function (Broca 1861) and is crucial in all classical and newly developed neurobiological models of language (see review by Price 2000). For a long time, Broca's area was taken as 1 single unit for language processing (Nishitani et al. 2005). However, its anatomical and functional segregation has recently become a focus of attention.

Traditionally, Broca's area comprises Brodmann's cytoarchitectonic areas (BA) 44 and 45, which occupy the left pars opercularis (l-oper) (BA 44) and left pars triangularis (l-tri)

(BA 45) of the inferior frontal gyrus. Owing to its fundamental role in language processing, especially in semantic processing (Bookheimer 2002; Devlin et al. 2003; Hagoort et al. 2004), left BA 47 (which occupies the left pars orbitalis [l-orb] of the inferior frontal cortex) has recently been included as a new member of "Broca's complex." Thus, in this paper, we will use Broca's complex to refer to the left inferior frontal language area (including BA 44, 45, and 47) following the proposal of Hagoort (Hagoort 2005a).

The anatomical parcellation of Broca's complex has been described in several cytoarchitectonic and DTI studies recently. BA 44 contains a thin layer IV of small granular cells with pyramidal cells from deep layer III and upper layer V intermingled with those of layer IV (dysgranular); BA 45 has densely packed granular cells in layer IV (granular) (Amunts et al. 2004). BA 47 is suggested to be, like BA 45, part of the heteromodal component of the frontal lobe, known as the granular cortex (Hagoort 2005b). The subregions in Broca's complex were also found to have distinct external anatomical connections. Anwander et al. (2007) employed diffusion tensor magnetic resonance (MR) imaging to parcellate Broca's area by identifying cortical regions with mutually distinct and internally coherent connectivity patterns. Three subregions were discernible that were identified as putative BA 44, BA 45, and the deep frontal operculum. The connectivity-based separations were found to be aligned with the macroanatomically identified boundary.

A corresponding functional division inside Broca's complex was suggested by the functional neuroimaging studies employing language processing tasks. In his memory, unification, and control (MUC) model (see Hagoort 2005b), Hagoort proposed that 3 functional components are the core of language processing: memory, unification and control, and the contribution of Broca's complex to language processing can be specified in terms of unification operations. Broca's complex recruits lexical information, mainly stored in temporal lobe structures that are known to be involved in lexical processing, and unifies them into overall representations that span multiword utterances. Based on the meta-analysis in Bookheimer (2002), Hagoort (2005b) suggested a functionally defined anterior ventral to posterior dorsal gradient in the left inferior frontal gyrus (LIFG). That is to say, BA 44 and parts of BA 6 have a role in phonological processing; BA 44 and BA 45 contribute to syntactic processing; and BA 47 and BA 45 are involved in semantic processing. LIFG is thus suggested to be involved in at least 3 different domains of language processing with a certain level of specialization in different LIFG subregions.

However, direct and comprehensive evidence for the functional parcellation of Broca's complex has not been

demonstrated to date. Very recently, several DTI studies examined the functional division within Broca's complex and the perisylvian language networks by investigating the anatomical connections in this network (Catani et al. 2005; Glasser and Rilling 2008). Unfortunately, it is very difficult to relate the fibers unequivocally to a given area in the cerebral cortex because DTI tracks nerve fibers (white matter), and the current limitation of the resolution of DTI technique makes it very hard to locate the end point in the gray matter.

In the present research, we performed a resting-state functional connectivity study to directly investigate the functional correlations within the perisylvian language networks by seeding from 3 subregions of Broca's complex and their homologues in the right hemisphere. Resting-state functional connectivity magnetic resonance imaging (fcMRI) detects temporal correlations in spontaneous blood oxygen level–dependent signal oscillations at low frequency (<0.1 Hz) while subjects rest quietly in the scanner (Biswal et al. 1995; Gusnard and Raichle 2001). Other than the DTI technology, which investigates fibers in white matter, the resting-state fluctuations are well localized in gray matter and can be used for detecting functional coherence in the cerebral cortex. Distinct resting-state networks have been related to vision, language, executive processing, and other sensory and cognitive domains (Greicius et al. 2008). Furthermore, a recent comparison of resting-state brain activity in humans and chimpanzees found that humans differ from chimpanzees in showing higher levels of left-lateralized activity in frontal, temporal, and parietal regions involved in language and conceptual processing. This result suggested that resting-state activity can reflect the strengthened language function in human brain (Rilling et al. 2007).

To our knowledge, this is the first systematic resting-state connectivity study on the functional division of Broca's complex (including pars orbitalis) and perisylvian language networks. Our results show a clear topographical functional organization in Broca's complex along with left middle frontal, parietal, and temporal areas.

Materials and Methods

Subjects
Twelve right-handed healthy subjects (6 females, age range 27–37 years) were scanned, according to institutional guidelines of the local ethics committee (CMO protocol region Arnhem-Nijmegen, The Netherlands).

MR Imaging
Subjects underwent 1 functional magnetic resonance imaging (fMRI) resting-state scan on a 3-T Siemens Trio scanner, using an 8-channel phased array head coil (Invivo 8 Channel Head Array). Resting-state data were acquired by using gradient-echo echo planar imaging (EPI) with the following imaging parameters: time repetition (TR) = 1400 ms, flip angle = 67° to conform to the Ernst angle for this TR, time echo = 30 ms, 21 slices, slice thickness 5 mm (slice gap = 1 mm), matrix size 64 × 64, resolution 3.5 × 3.5 × 5.0 mm, 1030 volumes, bandwidth 1815 Hertz per pixel, scan time 25 min. A longer scan time (roughly 4 times longer than the settings commonly reported in the literatures on resting-state connectivity study) was adopted to improve the sensitivity of signals. During the resting-state scans, subjects were required to stay awake with their eyes closed while avoiding any structured mental operation. All subjects were asked to confirm that they had not fallen asleep during the investigation.

Resting-State Connectivity Analyses
Of the original 1030 fMRI volumes, the initial 6 were discarded to allow for T_1 relaxation effects. All the subsequent volumes were coregistered to each other and normalized to the EPI template using routines from SPM5 (Wellcome Department of Imaging Neuroscience, University College London, UK). Non-brain structures were removed from these volumes by the BET brain extraction function in FSL (fMRIB's Software Library, http://www.fmrib.ox.ac.uk/fsl). Finally, spatial smoothing was applied by using a Gaussian kernel of 5 mm full width at half maximum.

Six frontal regions (l-oper/right pars opercularis [r-oper], left/right pars triangularis [l-tri/r-tri], and l-orbi/right pars orbitalis [r-orbi]) were taken as regions of interest (ROIs) for seeding. To avoid any influence of the size of seed on the correlation results, seed regions of equal size were selected in each ROI using the 3D-VOI function of Mricron (http://www.sph.sc.edu/comd/rorden/mricron/index.html). Based on the automated anatomical labeling template, the seed pixels were selected by drawing 3 spheres (each with a radius of 2 mm) as close as possible to the center of each ROI in the Montreal Neurological Institute (MNI) standard space. The 3 spheres are adjacent to each other without overlap and together make 1 ROI with continuous space. The reason for using 3 spheres rather than 1 single volume of interest (VOI) for each ROI is that irregularities in the form of the anatomical regions can be better accommodated in this way. The mean time course of each seed region (i.e., from all 3 spheres) was computed. Then we correlated these time courses with all the voxels in the brain to see the functional connectivity pattern arising from each ROI. Significance corrections for multiple comparisons were performed using a false discovery rate (FDR) correction ($P < 0.05$) (Genovese et al. 2002). Resting-state fMRI data are known to be dominated by very low–frequency fluctuations. Hence, we filtered the time courses with a "Butterworth filter" (band pass: 0.01–0.1 Hz) prior to the correlation analysis.

The correlation analyses were conducted using a random effects model in a general linear model (GLM) framework in SPM5. We also included in the model the mean signal time course of the brain to exclude drift effects and the 6 motion parameters to avoid motion artifacts.

Quantitative Analysis on the Topology and Laterality of the Connectivity Pattern
Based on individual data, the average connectivity (with standard errors) of each of the 3 left seeds to each of the 3 regions that constituted the observed topographical connectivity pattern in the left middle frontal, parietal, and temporal lobes (see Fig. 2 and Results) was computed. Using the 3D-VOI function of Mricron (http://www.sph.sc.edu/comd/rorden/mricron/index.html), the regions were defined as a sphere (radius: 3 mm) centered around their peak voxels (the voxel with the strongest connectivity). The connectivity strength was represented by the β coefficient of the GLM regressor of the seed. A follow-up 1-way analysis of variance and post hoc comparisons were performed to evaluate if the difference in the connectivity strength among the 3 seeds in 1 region was significant. The same set of statistics was performed for the 3 right seeds and the right homologous regions in the right middle frontal, parietal, and temporal areas to inspect if a similar connectivity pattern existed in the right hemisphere. A Bonferroni correction with a threshold of $P < 0.05$ was applied to adjust for multiple comparisons.

A comparison of connectivity strength between left and right hemispheres was then performed by quantifying the laterality of the topographical connectivity pattern. First, the connectivity strength of each left seed (i.e., l-oper, l-tri, or l-orbi) to each "connected region" in the left hemisphere (i.e., left middle frontal gyrus [MFG], left parietal lobe, or left temporal lobe) was calculated for each subject. Note that here the connectivity strength of each seed to each connected region was represented by the strongest connectivity between the seed and the connected region. For example, the connectivity strength of l-oper to left temporal lobe was represented by the connectivity strength of l-oper to left superior temporal gyrus. Second, the connectivity strength of each right seed (i.e., r-oper, r-tri, or r-orbi) to each "homologous region" in the right hemisphere (i.e., right MFG, right parietal lobe, or right temporal lobe) was also calculated for each subject in the same way. Then the connectivity strength of each left

seed to each left connected region was contrasted with the connectivity strength of each right seed to each homologous region at group level by performing paired 2-tailed *t*-tests.

Results

General Connectivity Pattern of the 6 Seed Regions

All subjects confirmed that they did not fall asleep during the whole session of scanning. Upon connectivity analysis, significant correlations in the brain were found for all 6 seed regions. Figure 1 shows the connectivity maps of the 6 seeds. Table 1 (for l/r-oper), Table 2 (for l/r-tri), and Table 3 (for l/r-orbi) give the anatomical locations and MNI coordinates of the clusters showing significant correlations.

Of the 6 seeds, l-oper and r-oper have similar connectivity patterns throughout the brain. Both of them connected significantly with a large number of clusters in the frontal, parietal, occipital, and temporal lobes. L-tri and r-tri were found to have overlapping connectivity in both hemispheres (l-oper/r-oper/precentral gyrus, left posterior middle temporal gyrus [pMTG]/posterior inferior temporal gyrus [pITG], left insula, and right supramarginal gyrus [SMG]/postcentral gyrus), but l-tri showed significant correlation with many more and larger brain areas (as can be seen in Fig. 1 and Table 2). L-orbi was found to be correlated with many areas, including r-orbi, bilateral pars opercularis/triangularis, bilateral MFG, left

angular gyrus (AG), left inferior parietal lobule, bilateral pITG, left temporal pole, left insula, bilateral putamen, and left supplementary motor area (SMA). However, areas connected with l-orbi appeared much smaller than those connected with l-oper or l-tri. R-orbi only correlated with bilateral pars orbitalis and right MFG/superior frontal gyrus and caudate/putamen.

The Observed Topographical Connectivity Pattern of the 3 Left Seed Regions

When the connectivity maps of all the 6 seed regions were overlaid in 1 window, a structured gradient topography of the connectivity pattern of the 3 left seeds was found in left MFG, left temporal lobe, and left parietal lobe. But no topographical connectivity pattern was found for the 3 right seeds at the current threshold. Figure 2 shows the topographical gradient in the left frontal seed regions (around l-oper, l-tri, and l-orbi), left MFG, temporal, and parietal lobes.

Around the seeding area, all 3 left seeds show strong connectivity with the ROIs from which they originated (this is also indicated in Tables 1, 2, and 3). Overlap among the 3 connectivity maps was found in all 3 seed regions. Particularly, a substantial overlap between the connectivity maps of l-oper and l-tri was found inside pars triangularis.

In left MFG (approximately BA 8/6/46), l-oper shows significant correlation with the posterior superior part
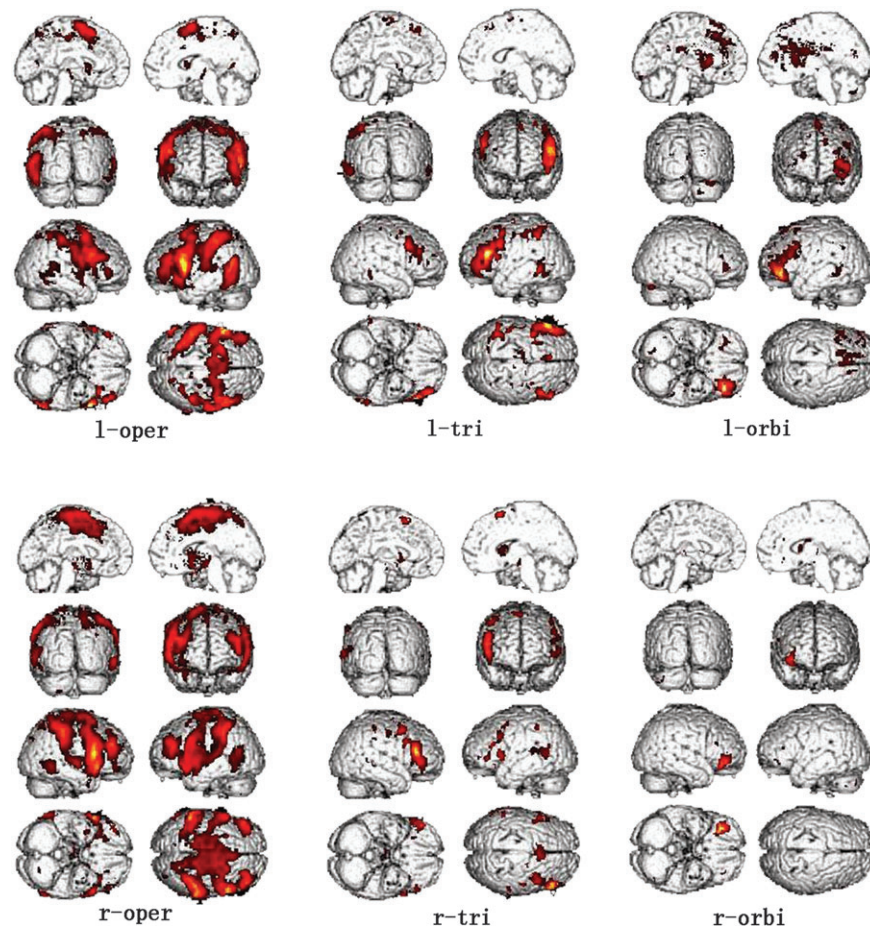
Figure 1. Resting-state connectivity pattern of 6 frontal seed regions across the whole group of subjects ($P \leq 0.05$ FDR corrected), overlaid on SPM5 standard brain in MNI space. L-oper, l-tri, l-orbi, r-oper, r-tri, and r-orbi represent the connectivity pattern to l-oper, l-tri, l-orbi, r-oper, r-tri, and r-orbi, respectively.

Table 1

Specification of clusters connected with l-oper/r-oper

	L-oper		R-oper	
	MNIp	Tp	MNIp	Tp
Left hemisphere				
Pars opercularis	−50, 13, 18	20.18	−52, 15, 8	5.53
Pars triangularis	−41, 36, 19	6.53	−44, 37, 22	8.19
Pars orbitalis	−45, 43, −14	4.33		
Precentral gyrus	−45, 10, 39	6.08	−54, 10, 36	8.82
MFG (BA 8/6)	−27, 9, 59	6.71	−33, 47, 28	5.82
SMG/postcentral gyrus	−47, −33, 58	7.98	−63, −39, 35	8.21
SMG/superior temporal gyrus	−63, −18, 17	8.38	−59, −30, 10	19.05
Superior/inferior parietal lobule (BA 7/40)	−38, −46, 56	6.13	−32, −49, 50	5.49
Posterior temporal lobe (BA 39/37/21/22)	−53, −64, 17	9.35	−59, −59, −3	4.50
Temporal pole	−50, 16, −16	5.75	−52, 16, −13	5.12
Insula/putamen	−38, 7, 3	5.05	−35, 0, −2	5.76
Right hemisphere				
Pars opercularis	49, 18, 33	6.85	54, 15, 13	20.64
Pars triangularis	52, 27, 29	6.44	40, 28, 25	4.11
Pars orbitalis	52, 40, −4	4.67	42, 46, −5	5.00
Precentral gyrus	50, 10, 48	7.09	49, 6, 43	5.73
MFG (BA 46)	40, 8, 56	5.16	45, 42, 26	9.47
Postcentral gyrus	57, −8, 30	5.39	19, −33, 64	4.35
SMG/postcentral gyrus	49, −31, 49	4.47	59, −32, 45	9.35
Superior/inferior parietal lobule (BA 7/40)	38, −49, 59	4.42	42, −52, 56	9.24
Occipital lobe cuneus (BA 19)	40, −74, 25	3.44	36, −79, 36	3.50
pSTG/pMTG	67, −42, 12	6.43		
pITG/pMTG (BA 37)	60, −51, −12	3.46	63, −55, −6	4.87
aSTG (BA 21)	60, −2, −8	5.74	58, −9, 1	4.40
Insula/putamen	43, −6, 1	3.70	37, 17, −10	9.18
SMA	6, 15, 52	6.44	2, 17, 55	7.48

Note: For each cluster, the MNI coordinate (MNIp) and T value (Tp) of the peak voxel and the anatomical location are given. The threshold used is $P < 0.05$, FDR corrected (cluster criterion: 5 voxels). aSTG, anterior superior temporal gyrus.

Table 2

Specification of clusters connected with l-tri/r-tri

	L-tri		R-tri	
	MNIp	Tp	MNIp	Tp
Left hemisphere				
Pars triangularis	−48, 30, 20	19.43	−43, 28, 19	6.44
Pars opercularis	−41, 13, 34	8.36	−55, 15, 8	6.46
Precentral gyrus			−49, 14, 38	6.64
Pars orbitalis	−46, 41, −4	5.60		
MFG (BA 6)	−38, 5, 53	6.00		
MFG (BA 8/9)	−26, 12, 61	5.00		
SMG/postcentral gyrus	−45, −30, 51	5.07		
Superior/inferior parietal lobule (BA 7/40)	−50, −47, 49	7.13	−56, −41, 48	7.43
pMTG/pITG (BA 37/21)	−57, −48, −6	5.64	−62, −56, 9	6.67
Insula	−31, 25, 0	4.80		
Putamen	−20, 1, −2	4.34	−13, 8, 3	5.38
Right hemisphere				
Pars triangularis	55, 33, 24	7.81	52, 30, 18	17.71
Pars opercularis	43, 15, 36	7.93	43, 15, 34	5.73
Precentral gyrus			47, 10, 51	7.69
MFG (BA 8/6)	36, 4, 57	6.00		
Pars orbitalis			29, 28, −14	5.0
SMG/postcentral gyrus			62, −42, 36	4.19
Lateral middle/temporal gyrus (BA 20/21)	64, −44, −2	5.60		
pMTG (BA 37)			60, −44, 5	4.54
Caudate/putamen			17, 7, 12	4.85
SMA	−4, 30, 57	5.90	8, 16, 63	7.30

Note: For each cluster, the MNI coordinate (MNIp) and T value (Tp) of the peak voxel and the anatomical location are given. The threshold used is $P < 0.05$, FDR corrected (cluster criterion: 5 voxels).

Table 3

Specification of clusters connected with l-orbi/r-orbi

	L-orbi		R-orbi	
	MNIp	Tp	MNIp	Tp
Left hemisphere				
Pars orbitalis	−35, 41, −4	12.09	−34, 38, −7	6.00
Pars opercularis/triangularis (BA 44/45/48)	−32, 26, 26	5.78		
MFG (BA 46)	−31, 37, 19	6.19		
MFG (BA 8)	−30, 21, 31	7.23		
AG	−38, −54, 34	5.57		
pITG (BA 37/20)	−46, −47, −4	5.06		
Temporal pole	−36, 27, −24	4.48		
Caudate/putamen	−15, 17, 16	7.24		
Right hemisphere				
Pars orbitalis	38, 40, 5	5.61	34, 38, −3	20.87
MFG/SFG (BA 48/46)			31, 45, 7	7.78
MFG (BA 46)	21, 19, 31	4.79		
pMTG (BA 37)	41, −28, −3	4.76		
Caudate/putamen	19, 14, 7	5.01	15, 6, 10	6.04
SMA	−2, 30, 61	5.42		

Note: For each cluster, the MNI coordinate (MNIp) and T value (Tp) of the peak voxel and the anatomical location are given. The threshold used is $P < 0.05$, FDR corrected (cluster criterion: 5 voxels). SFG, superior frontal gyrus.

(approximately BA 8/6), whereas l-orbi exhibits a significant correlation with the anterior inferior part (approximately BA 46). The area connected with l-tri lies between areas connected with l-oper and l-orbi and has a large overlap with the region connected with l-oper and small overlap with the region connected with l-orbi.

In left parietal lobe, l-oper correlates with the superior and anterior parts of the superior and inferior parietal lobules, SMG, and postcentral gyrus. L-orbi correlates with the posterior and inferior parts of the superior and inferior parietal lobules (adjacent to and overlapping with AG). The area connected with l-tri lies right between the connectivity maps of l-oper and l-orbi in the superior and inferior parietal lobules, with a large overlap with the area connected with l-oper.

In left temporal lobe, l-oper correlates largely with the posterior superior temporal gyrus (pSTG) and the superior part of the pMTG and also extends to pITG. L-tri correlates with pMTG and extends to pSTG and pITG, which overlaps with and is somewhat inferior to those areas connected with l-oper. L-orbi only correlates with pITG, which lies in the most inferior part of the temporal region.

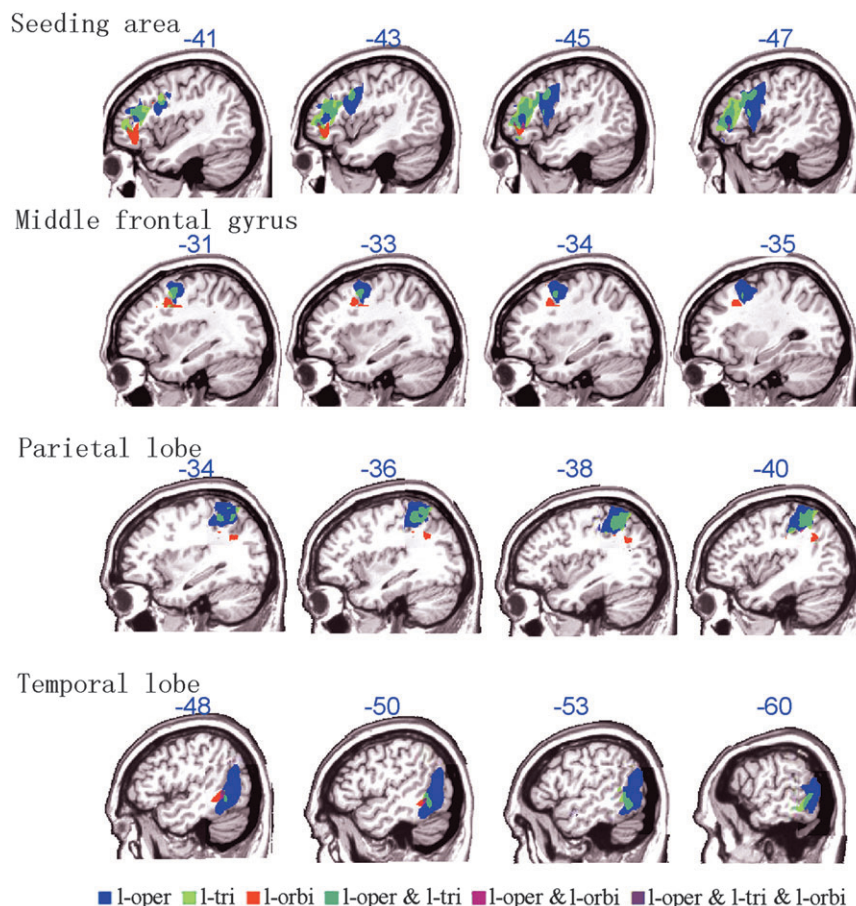A sketch of the topographical connectivity pattern can be seen in Figure 3a.

The Quantitative Topology and Laterality of the Topographical Connectivity Pattern

In Figure 3b, the average connectivity (with standard errors) of each of the 3 left seeds to each of the 3 regions that constituted the observed topographical connectivity pattern in the left middle frontal, parietal, and temporal lobes is presented. Significant differences in the connectivity strength between l-oper and each of the other 2 left seeds were found in T1 (pSTG and superior pMTG). Similar significant differences were found between l-orbi and each of the other 2 left seeds in T3 (pITG). In M1 (the anterior inferior part of MFG), P1 (superior and anterior part of the superior and inferior parietal lobules), M3 (the posterior superior part of MFG), and P3 (area adjacent to and overlapping with AG), significant differences were

Figure 2. The topographical connectivity pattern in frontal, temporal, and parietal lobes of the 3 left seeds. L-oper, l-tri, and l-orbi represent the connectivity pattern to l-oper, l-tri, and l-orbi, respectively. "&" Indicates the overlapping connectivity pattern to the 2 or 3 seeds. Above each image, the MNI coordinate index is shown in blue. For the sake of a better presentation, the threshold for the connectivity map of seeding area is set to $P < 0.02$ FDR corrected, which is a little bit more conservative than the threshold used for the connectivity map of left MFG, temporal lobe, and parietal lobe ($P < 0.05$ FDR corrected).

detected between l-oper and l-orbi. Although all the other comparisons were not significantly different, the average connectivity of each seed to those regions showed a gradient consistent with the topographical connectivity pattern shown in Figure 2 and depicted in Figure 3a. In M3, P1, and T1, l-oper shows the highest average connectivity; l-tri shows less; and l-orbi is the lowest. In M1, P3, and T3, on the contrary, l-orbi shows the highest average connectivity; l-tri shows less; and l-oper is the lowest. While in M2 (the MFG area between M1 and M3), P2 (the area between P1 and P3 in the superior and inferior parietal lobules), and T2 (inferior pMTG), l-tri shows the highest average connectivity; l-oper shows less; and l-orbi is the lowest.

In the right hemisphere (see Fig. 4), a similar gradient of the average strength was observed only in M3, P1, and T3. Significant differences were detected between r-oper and each of the other 2 right seeds in M3 and P1.

The results of the comparison of the connectivity strength between left and right hemispheres are shown in Table 4. The connectivity between pars opercularis and posterior temporal lobe (to be more precise, pSTG and the superior part of pMTG) and the connectivity between pars orbitalis and parietal lobe (adjacent to and overlapping with AG) in the left hemisphere are significantly stronger than those in the right hemisphere.

Discussion

Explanation for General Connectivity Patterns

Seeding from Broca's complex, significant correlations were found to many brain regions including, but not exclusively, the traditional perisylvian language loop (see Tables 1, 2, and 3). Broca's area has been suggested to have a central role in coordinating time-sensitive perceptual and motor functions underlying verbal and nonverbal communication and is involved in various functions (see review by Judas and Cepanec 2007). Thus, it is not surprising to find significant connectivity not only to previously suggested phonological, syntactic, and semantic areas (such as pSTG/pMTG/pITG, SMG, AG, and insula) but also to the sensory/motor areas (such as pre/postcentral gyrus, SMA, and caudate/putamen).
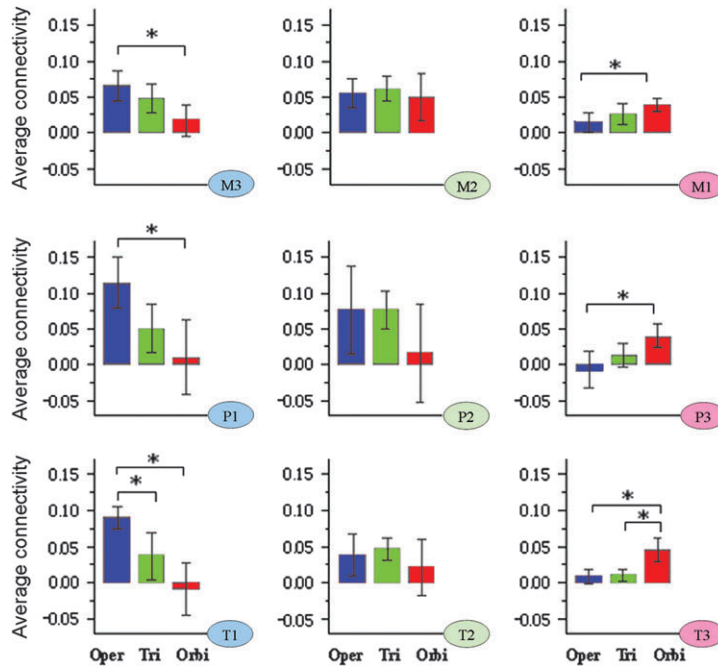
The Left Topographical Connectivity Pattern and Its Functional Division

What is most interesting among the present results is the topographical connectivity pattern of Broca's complex within the left middle frontal, parietal, and temporal areas. This functional connectivity result is consistent with the results of previous functional language studies.
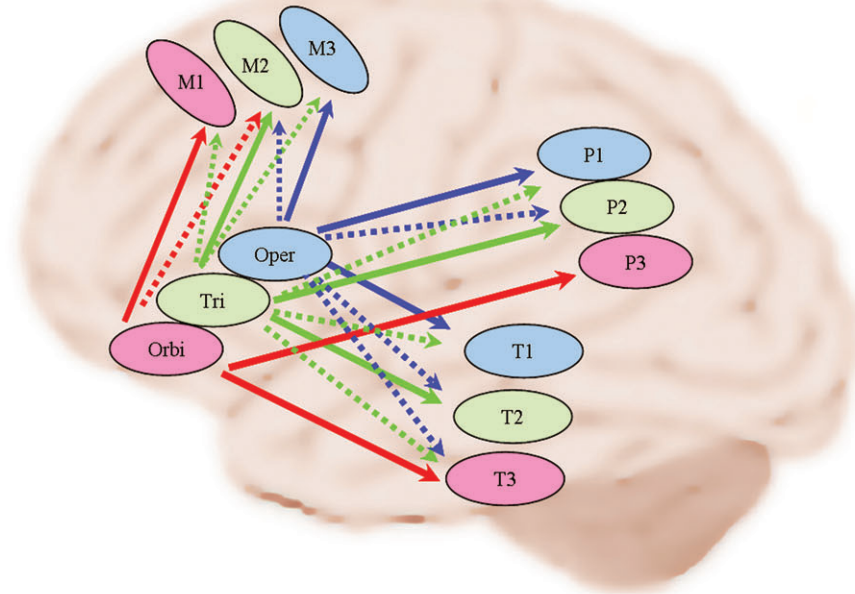
Figure 3. *a*) The topographical connectivity pattern in the perisylvian language networks. Connections to l-oper (oper), l-tri (tri), and l-orbi (orbi) are shown with blue, green, and red arrows, respectively. The solid arrows represent the highest connectivity, and the dashed arrows represent the overlapping connections. Brain areas assumed to be mainly involved in phonological, syntactic, and semantic processing are shown in light blue, light green, and light red circles, respectively (for details on the function and interaction of these brain areas, refer to the Discussion). (*b*) The average connectivity (with standard errors) of each of the 3 left seeds to each of the 3 regions that constituted the observed topographical connectivity pattern in the left middle frontal, parietal, and temporal lobes. M1, the anterior inferior part of MFG; M3, the posterior superior part of MFG; M2, the MFG area between M1 and M3; P1, superior and anterior part of the superior and inferior parietal lobules; P3, area adjacent to and overlapping with AG; P2, the area between P1 and P3 in the superior and inferior parietal lobules; T1, pSTG and superior pMTG; T2, inferior pMTG; T3, pITG. Oper, Tri, or Orbi represent each of the 3 left seeds. "*" Indicates significant difference ($P < 0.05$ Bonferroni corrected) in the connectivity strength between 2 seeds in that brain region.

We used Broca's complex (including pars orbitalis) instead of the traditional Broca's area as our seed regions in the present study because pars orbitalis has been found to play an important role in language (especially semantic) processing. As reviewed by Hagoort et al. (forthcoming), the activation of BA 47 and BA 45 has been consistently found to be activated across semantic studies employing different design paradigms.

These studies either compared sentences containing semantic/pragmatic anomalies with their correct counterparts (Kuperberg et al. 2000, 2003, 2008; Ni et al. 2000; Newman et al. 2001; Friederici et al. 2003; Hagoort et al. 2004; Ruschemeyer et al. 2005) or compared sentences with and without semantic ambiguities (Hoenig and Scheef 2005; Rodd et al. 2005; Davis et al. 2007; Zempleni et al. 2007).
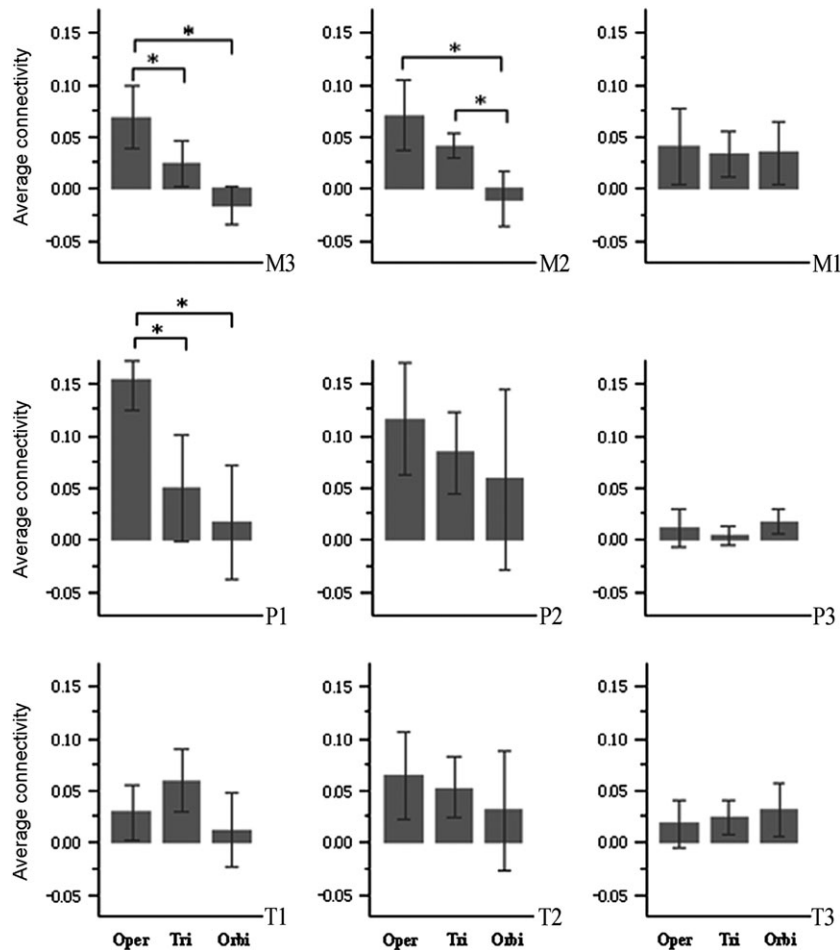
Figure 4. The average connectivity (with standard errors) of each of the 3 right seeds to each of the 3 right homologous regions in the right middle frontal, parietal, and temporal lobes. M1, the anterior inferior part of MFG; M3, the posterior superior part of MFG; M2, the MFG area between M1 and M3; P1, superior and anterior part of the superior and inferior parietal lobules; P3, area adjacent to and overlapping with AG; P2, the area between P1 and P3 in the superior and inferior parietal lobules; T1, pSTG and superior pMTG; T2, inferior pMTG; T3, pITG. Oper, Tri, or Orbi represent each of the 3 right seeds. "*" Indicates significant difference of the connectivity strength between 2 seeds in that brain region.

Table 4

The contrasts of connectivity between left and right hemisphere

	Middle frontal		Posterior temporal		Parietal lobe	
	T	P	T	P	T	P
Oper	−0.24	0.82	3.58*	0.004	−2.02	0.07
Tri	1.96	0.08	−0.38	0.71	−0.31	0.76
Orbi	0.42	0.68	1.34	0.21	2.85*	0.02

Note: T and P represent the T value and P value of the 2-tailed paired t-test, respectively. A positive T value indicates stronger connectivity in the left hemisphere than in the right hemisphere. A negative T value means weaker connectivity in the left hemisphere than in the right hemisphere.

*Significant results ($P < 0.05$).

As mentioned in the Introduction, the MUC model suggested an anterior ventral to posterior dorsal functional gradient in Broca's complex: BA 44 for phonological processing, BA 44 and BA 45 for syntactic processing, and BA 47 and BA 45 for semantic processing. The assumption was mainly based on the recent meta-analysis of neuroimaging language studies by Bookheimer (2002). However, the observation of similar results in language studies is not new. Poldrack et al. (1999) conducted a literature search in an attempt to find all brain imaging studies employing task comparisons designed to isolate semantic, phonological, or lexical processing. They characterized each task comparison in terms of several different categories: semantic decision (e.g., living–nonliving decision), semantic production (e.g., verb generation), lexical retrieval (i.e., word/nonword decision and word-stem completion), phonological processing (e.g., phoneme monitoring or nonword processing), overt speech (e.g., word repetition or naming), and silent viewing of words. Their review demonstrated that the posterior and dorsal regions of the left inferior frontal cortex (corresponding to BA 44/45) were specialized for phonological processing, and the ventral and anterior regions of the left inferior frontal cortex (approximating to BA 47/45) were preferentially active during the performance of tasks requiring overt semantic processing. Besides these brain imaging studies, direct cortical stimulation of area 44 in patients undergoing surgical removal of the epileptic focus disrupts phoneme monitoring even when patients were not

required to articulate (Ojemann and Mateer 1979). Another study using chronically implanted depth electrodes in BA 47 found greater activity in that region related to semantic decision relative to a perceptual decision (Abdullaev and Bechtereva 1993). Existing results on the study of syntactic processing highlight the role of pars triangularis for syntax. Musso et al. (2003) reviewed the studies on syntactic processing in their discussion and concluded that pars triangularis has an "indisputable and essential" function for the processing of syntactic aspects of language. Because activation in pars triangularis in syntactic processing was found to be independent of the language (English, Chinese, German, Italian, or Japanese) of subjects (Hahne and Friederici 1999; Embick et al. 2000; Friederici et al. 2000; Ni et al. 2000; Sakai et al. 2002), they suggested that this brain region is specialized for the acquisition and processing of hierarchical (rather than linear) structures, which represents the common character of every known grammar. Furthermore, a meta-analysis of functional neuroimaging studies of syntactic processing (Indefrey 2004) reported that the most replicable finding related to syntactic parsing across imaging techniques, presentation modes, and experimental procedures was the activation localized in left BA 44 and BA 45, consistent with what is known from brain lesion data (Caramazza and Zurif 1976; Friederici 2002).

Thus, by seeding from the 3 subregions of Broca's complex in this study, we expected to discover a connectivity pattern that is consistent with these previous results: pars opercularis (corresponding to BA 44) mainly correlates with brain areas for phonological processing and also extends to brain regions for syntactic processing, pars triangularis (corresponding to BA 45) mainly correlates with brain areas for syntactic processing and also extends to brain regions for phonological and semantic processing, whereas pars orbitalis mainly correlates with brain regions involved in semantic processing. Our results are indeed consistent with those assumptions. Details are given in the following paragraphs.

In left temporal lobe, l-oper correlates largely with pSTG and the superior part of pMTG and also extends to pITG. L-tri correlates with pMTG and extends to pSTG and pITG, which overlaps with and is somewhat inferior to those areas connected with l-oper. L-orbi only correlates with pITG. In functional neuroimaging studies, activations related to phonological/phonetic properties have been mostly reported for the central to posterior STG extending into the superior temporal sulcus (Binder 1997; Binder et al. 2000; Cannestra et al. 2000; Castillo et al. 2001; Jancke et al. 2002; McDermott et al. 2003; Scott and Johnsrude 2003; Aleman et al. 2005; Indefrey and Cutler 2005; Papanicolaou et al. 2006) and activations related to semantic information have been mostly found to be distributed in the left middle and inferior temporal gyri (Damasio et al. 1996; Vandenberghe et al. 1996; Binder 1997, 2000; Saffran and Sholl 1999; Cannestra et al. 2000; Price 2000; Billingsley et al. 2001; Castillo et al. 2001; Hickok and Poeppel 2004; Poeppel et al. 2004; Gitelman et al. 2005; Indefrey and Cutler 2005). Although the neural substrates of syntactic processing within the temporal lobe have not been consistently located, pMTG has been shown to be activated in syntactic tasks and supports processing of sentence structure (Stowe et al. 1998; Cooke et al. 2002; Constable et al. 2004; Snijders et al. 2008). Besides, activation of pSTG has also been found in relation to syntactic complexity (Constable et al. 2004) and grammatical violation (Embick et al. 2000).

Recently, Hagoort et al. (forthcoming) suggested an interesting distinction of function between superior temporal and inferior frontal areas. The superior temporal gyrus was observed to have a higher activation level in response to a congruent sound and image/letter combination as compared with an incongruent combination (Beauchamp et al. 2004; Van Atteveldt et al. 2004; Hein et al. 2007), whereas inferior frontal area showed a stronger response when matching incongruent sounds and images/letters (Hein et al. 2007). It was argued that these results suggested a possible division of labor between inferior frontal and superior temporal areas, with a stronger contribution to integration for superior/middle temporal cortex and a stronger role for the inferior frontal cortex in unification. Integration occurs when different sources of information converge to a common memory representation. This part of the cortex is more strongly involved in conditions with a congruent input, resulting in converging support for a pre-stored representation. Unification refers to a constructive process in which a semantic or syntactic representation is constructed that is not already available in memory. This is always harder for more complex or incongruous input (Hagoort et al. forthcoming). Combining these previous functional neuroimaging results and the present connectivity results, we suggest that the unification component for each linguistic modality (phonology, syntax, or semantics) in the inferior frontal cortex has a corresponding integration/memory component in the posterior temporal cortex, and these 2 corresponding components are highly correlated with each other. To summarize, posterior superior/middle temporal cortex and pars opercularis (mainly)/triangularis for phonological integration and unification, respectively; posterior middle temporal cortex and pars triangularis (mainly)/opercularis for syntactic integration and unification, respectively; posterior inferior (mainly)/middle temporal cortex and pars orbitalis (mainly)/pars triangularis for semantic integration and unification, respectively. This connectivity pattern is illustrated in Figure 3a.

In left parietal lobe, l-oper was found to be correlated with both SMG and the postcentral gyrus. L-orbi mainly correlated with the brain regions adjacent to and overlapping with AG. The area connected with l-tri lies right between the connectivity maps of l-oper and l-orbi in the superior and (mainly) inferior parietal lobules. Patients with left parietal lesions have been noted to have deficits in auditory short-term memory (Warrington and Shallice 1969; Saffran and Marin 1975). Functional imaging studies have implicated the same area in tasks accessing the phonological store in working memory (Jonides et al. 1998; Cabeza and Nyberg 2000). Particularly, the function of left parietal lobe for phonological processes (e.g., mapping orthography to phonology, phonological recoding, rhyme detection, etc.) seems mainly to involve SMG (Demonet et al. 1992, 1994; Paulesu et al. 1993; Price 1998; Pugh et al. 2001; Seghier et al. 2004). In contrast, AG has been observed to be mostly involved in semantic processing (Demonet et al. 1993, 1994; Binder 1997; Lurito et al. 2000; Price 2000; Binder et al. 2005; Sabsevitz et al. 2005). Lesion studies of patients with alexia have proposed that the posterior portion of the reading network in the left cerebral hemisphere involves functional links between AG and extrastriate areas in occipital and temporal cortices associated with the visual processing of letter and word-like stimuli. AG is also thought to have functional links with posterior language areas (e.g., Wernicke's area) and is presumed to be involved in mapping visually

presented inputs onto linguistic representations (see review by Horwitz et al. 1998). Few reports have been published on the syntactic function of the parietal lobe. However, a parietal area responsible for the omission of syntactic–morphological markers has been consistently identified in 2 patients in a cortical electrical stimulation mapping study (Bhatnagar et al. 2000). This parietal area is presumably in the region between SMA and AG (see Figs 1 and 2 in Results of Bhatnagar et al. 2000), though the authors did not precisely name it in their report. A functional neuroimaging study (Embick et al. 2000) also found a so-called "AG/SMG" region, which was more activated by ungrammatical sentences than sentences containing spelling errors. The coordinates reported by the authors for the center of this AG/SMG region lie right inside the parietal area connected with l-tri in the present study. Combining previous research with our functional connectivity results again shows the similar topographical connectivity pattern in left parietal lobe: l-oper is mainly correlated with brain areas for phonological processing (SMG) and l-orbi is correlated with brain regions for semantic processing (AG). Based on the reports from the cortical electrical stimulation mapping and neuroimaging studies, we hypothesize that the areas connected with l-tri in the superior and inferior parietal lobules may have a function in syntactic processing. Further precisely designed studies are needed to test this hypothesis.

The topographical connectivity pattern and its functional division in the parietal lobe suggest a different explanation for the Geschwind's territory that was discovered by Catani et al. (2005) in their DTI study on perisylvian language connectivity. Beyond the classical arcuate pathway connecting Broca's and Wernicke's areas directly, they found an indirect pathway passing through a region of inferior parietal cortex, which they called the Geschwind's territory. Catani et al. (2005, 2007) interpreted the indirect pathway and the Geschwind's territory as subserving semantic processing. However, their figures (mainly Fig. 2) show that the focus of the so called Geschwind's territory is in SMG, which in the present results, along with pSTG, shows a very strong connectivity to l-oper. Thus, the present results suggest that the Geschwind's territory is more likely to be involved in phonological rather than semantic processing.

In left MFG, l-oper has significant connectivity with the posterior superior part (approximately BA 8/6), l-orbi shows significant correlation with the anterior inferior part (approximately BA 46), whereas l-tri mainly reveals strong connectivity in the middle part (between areas connected with l-oper and l-orbi). MFG (approximately BA 8/6/46) is also known as the dorsolateral prefrontal cortex (DLPFC) and has been associated with aspects of executive control. Activations of this area are typically observed in tasks that require maintenance and manipulation of information in working memory (for a review, see Miller 2000). In the language domain, it has been found to be involved in verbal action planning and intentional control (Roelofs and Hagoort 2002) and the control of language switching in bilinguals (Abutalebi et al. 2008; van Heuven et al. 2008). However, little is known about the functional division of MFG from language studies. Based on the connectivity pattern in the left temporal and parietal lobes, our results tentatively suggest that MFG is also topographically organized and displays a gradient of functional organization in which the posterior superior MFG is more involved in phonological control, the anterior inferior MFG is more involved in semantic control, and

the middle part between the 2 areas is more involved in syntactic control. In spite of sparse evidence from language research, the functional division of MFG has been mainly studied in researches on cognitive control. Based on the research results in this field, Koechlin et al. (2003) proposed a cascade model on the architecture of cognitive control in the lateral prefrontal cortex (LPFC). This model postulated that the LPFC was organized as a hierarchy of representations and processed distinct signals involved in controlling the selection of appropriate stimulus–response associations. Specifically, it hypothesized that cognitive control involved at least 3 nested levels of processing, implemented in distinct LPFC regions. Interestingly, the topographical connectivity pattern in MFG in the present study reveals a similar corresponding hierarchical anatomy as the suggested architecture in LPFC for the 3 levels of cognitive control in the cascade model. This may indicate a close correspondence between the general cognitive function and the specific language processing in MFG. Given that fcMRI can probe connectivity, but not function, we do not wish to make any specific claims regarding the functional division of MFG.

It should be noticed that there is much overlap between the connectivity patterns of the 3 seed regions, even though the foci of the connectivity maps are separable. In the present results, overlap of the connectivity pattern can be found inside Broca's complex itself and also in the left middle frontal, parietal, and temporal lobes where the topographical connectivity pattern was found. This is consistent with previous results of functional imaging studies. Bookheimer (2002) has concluded in her review article that the subregions of the inferior frontal gyrus form a network of unique but highly interactive, compact modules, which give rise to the tremendously complex language processing of which humans are capable. The MUC model also claims that the overlap of activations for the 3 different types of information is substantial and suggests the possibility of interactive concurrent processing in which various types of processing constraints are incorporated as soon as they become available. Particularly, in the topographical connectivity pattern found in the present study, the connectivity pattern of l-tri was always found to have a large overlap with that of l-oper, which suggests substantial functional interactions between these 2 regions. Several DTI studies consistently report that both l-oper and l-tri connect with parietal and temporal association cortices by a dorsal pathway via the arcuate and the superior longitudinal fasciculi (Catani et al. 2005; Anwander et al. 2007). However, l-orbi seems to be connected to temporal cortex by a ventral pathway via the uncinate fascicle (Anwander et al. 2007). Figure 3a summarizes the topographical connectivity pattern and those interactions in Broca's complex, MFG, parietal lobe, and temporal lobe.

It is also interesting to notice that the main findings of the present study can be interpreted within the framework of the MUC model (Hagoort 2005b). As being mentioned in the Introduction, the MUC model suggested 3 functional components to be the core of language processing: memory, unification and control Broca's complex is proposed as the "unification area" and is thought to be at the heart of the combinatorial nature of language. Unification refers to the integration of lexically retrieved information into a representation of multiword utterances and the integration of meaning extracted from nonlinguistic modalities. The memory component refers to the different types of language information

stored in long-term memory and the retrieval operations, which includes the phonological/phonetic properties of words, their syntactic features, and their conceptual specifications. The left temporal lobe was suggested to be the "memory area." The control component was assumed to account for the fact that the language system operates in the context of communicative intentions and actions and was suggested to have a neural base in MFG (DLPFC) and anterior cingulate cortex. In the present research, we do discover a strong correlation to the memory area and the "control area" (MFG in the present study) by seeding from the unification area. And the connectivity pattern in the memory area and the control area is consistently topographically and functionally organized according to the subregions we seeded in the unification area. This is also consistent with the functional division as what has been suggested in the model itself. However, our results revealed that the parietal lobe also correlated strongly with the unification area, but its involvement in the language processing is not yet described by the MUC model.

The Different Strength of the Connectivity Pattern

In both hemispheres, the largest connectivity pattern was observed for pars opercularis and the smallest connectivity pattern was seen for pars orbitalis. Pars triangularis showed less connectivity than pars opercularis but more than that of pars orbitalis. This difference in connectivity strength is not likely to be caused by the size of seed regions because equal seed regions were selected in each region in the present research. The percentage of white/gray matter included in the seed regions also is not likely to affect the results because we chose the seeds from the central region of each ROI and computed the mean time courses of each seed region for the correlation analysis. Thus, this difference in connectivity strength seems to reflect the intrinsic differences in the strength of the functional connections in the perisylvian language networks. Consistently, it is interesting to notice that several recent DTI studies on language networks discovered strong anatomical connections among SMG, Broca's area, and Wernicke's area (Catani et al. 2005; Parker et al. 2005), which could well correspond to our connectivity pattern for pars opercularis (maybe also partly correspond to the connectivity pattern for pars triangularis because there is great overlap between the connectivity pattern of pars opercularis and pars triangularis). However, to our knowledge, no such report on the connection among pars orbitalis, AG, and pITG has been made.

The Laterality of the Connectivity Pattern

When the connectivity maps of all the 6 seed regions were overlaid in 1 window, the structured gradient topography of the connectivity pattern was only found in the left hemisphere. No such topographical connectivity pattern was found in the right hemisphere at the threshold we used (FDR corrected $P <$ 0.05). Further comparisons of the strength of the topographical connectivity pattern between the 2 hemispheres revealed several significant differences. The connectivity between pars opercularis and the temporal lobe (particularly, pSTG) and the connectivity between pars orbitalis and the parietal lobe (particularly, AG) in the left hemisphere were significantly stronger than those in the right hemisphere. Greater fronto-temporal connectivity on the left has been found by Powell et al. (2006) when they used MR tractography to demonstrate

the structural connections of the cortical regions activated by expressive and receptive language tasks. They proposed that this structural asymmetry reflects the left-sided lateralization of language function in the human brain.

As a whole, the left-lateralized topographical connectivity pattern probably suggests that the left hemisphere layout follows a more functionally parcellated segregation of language function than the right hemisphere.

Conclusion

We used fcMRI to infer the functional organization of Broca's complex and the perisylvian language networks by investigating their functional correlations. A clear topographical functional connectivity pattern in the left middle frontal, parietal, and temporal areas was revealed when seeding from the 3 subregions (pars opercularis, pars triangularis, and pars orbitalis) of Broca's complex. The results are consistent with previous studies on the language function of brain. They support the assumption of the functional division for phonology, syntax, and semantics of Broca's complex as proposed by the MUC model and indicated a topographical functional organization and division of labor for phonological, syntactic, and semantic function in the left frontal, parietal, and temporal areas.

Notes

References

Abdullaev YG, Bechtereva NP. 1993. Neuronal correlate of the higher-order semantic code in human prefrontal cortex in language tasks. Int J Psychophysiol. 14:167–177.

Abutalebi J, Annoni JM, Zimine I, Pegna AJ, Seghier ML, Lee-Jahnke H, Lazeyras F, Cappa SF, Khateb A. 2008. Language control and lexical competition in bilinguals: an event-related fMRI study. Cereb Cortex. 18:1496-1505.

Aleman A, Formisano E, Koppenhagen H, Hagoort P, Edward HFH, Kahn RS. 2005. The functional neuroanatomy of metrical stress evaluation of perceived and imagined spoken words. Cereb Cortex. 15:221-228.

Amunts K, Weiss PH, Mohlberg H, Pieperhoff P, Eickhoff S, Gurd J, Shah JN, Marshall JC, Fink GR, Zilles K. 2004. Analysis of the neural mechanisms underlying verbal fluency in cytoarchitectonically defined stereotactic space—the role of Brodmann's areas 44 and 45. Neuroimage. 22:42-56.

Anwander A, Tittgemeyer M, von Cramon DY, Friederici AD, Knosche TR. 2007. Connectivity-based parcellation of Broca's area. Cereb Cortex. 17(4):816-825.

Beauchamp MS, Lee KE, Argall BD, Martin A. 2004. Integration of auditory and visual information about objects in superior temporal sulcus. Neuron. 41:809-823.

Bhatnagar SC, Mandybur GT, Buckingham HW, Andy OJ. 2000. Language representation in the human brain: evidence from cortical mapping. Brain Lang. 74(2):238-259.

Billingsley RL, McAndrews MP, Crawley AP, Mikulis DJ. 2001. Functional MRI of phonological and semantic processing in temporal lobe epilepsy. Brain. 124(6):1218-1227.

Binder J. 1997. Functional magnetic resonance imaging: language mapping. Neurosurg Clin N Am. 8(3):383-392.

Binder JR, Frost JA, Hammeke TA, Bellgowan PS, Springer JA, Kaufman JN, Possing ET. 2000. Human temporal lobe activation by speech and nonspeech sounds. Cereb Cortex. 10:512-528.

Binder JR, Medler DA, Desai R, Conant LL, Liebenthal E. 2005. Some neurophysiological constraints on models of word naming. Neuroimage. 27:677-693.

Biswal B, Yetkin FZ, Haughton VM, Hyde JS. 1995. Functional connectivity in the motor cortex of resting human brain using echo-planar MRI. Magn Reson Med. 34:537-541.

Bookheimer S. 2002. Functional MRI of language: new approaches to understanding the cortical organization of semantic processing. Annu Rev Neurosci. 25:151-188.

Broca P. 1861. Remarques sur le siége de la faculté du langage articulé, suivies d'une observation d'aphémie (perte de la parole). Bulletin de la Société Anatomique de Paris. 6:330-357.

Cabeza R, Nyberg L. 2000. Imaging cognition II: an empirical review of 275 PET and fMRI studies. J Cogn Neurosci. 12(1):1-47.

Cannestra AF, Bookheimer SY, Pouratian N, O'Farrell A, Sicotte N, Martin NA, Becker D, Rubino G, Toga AW. 2000. Temporal and topographical characterization of language cortices using intraoperative optical intrinsic signals. Neuroimage. 12:41-54.

Caramazza A, Zurif E. 1976. Dissociation of algorithmic and heuristic processes in language comprehension: evidence from aphasia. Brain Lang. 3:572-582.

Castillo EM, Simos PG, Davis RN, Breier J, Fitzgerald ME, Papanicolaou AC. 2001. Levels of word processing and incidental memory: dissociable mechanisms in the temporal lobe. Neuroreport. 12:3561-3566.

Catani M, Allin MPG, Husain M, Pugliese L, Mesulam MM, Murray RM, Jones DK. 2007. Symmetries in human brain language pathways correlate with verbal recall. Proc Natl Acad Sci USA. 104(43):17163-17168.

Catani M, Jones DKJ, ffytche DH. 2005. Perisylvian language networks of the human brain. Ann Neurol. 57:8-16.

Constable RT, Pugh KR, Berroya E, Mencl WE, Westerveld M, Ni W, Shankweiler D. 2004. Sentence complexity and input modality effects in sentence comprehension: an fMRI study. Neuroimage. 22:11-21.

Cooke A, Zurif EB, DeVita C, Alsop D, Koenig P, Detre J, Gee J, Pinango M, Balogh J, Grossman M. 2002. Neural basis for sentence comprehension: grammatical and short-term memory components. Hum Brain Mapp. 15:80-94.

Damasio H, Grabowski TJ, Tranel D, Hichwa RD, Damasio AR. 1996. A neural basis for lexical retrieval. Nature. 381:810.

Davis MH, Coleman MR, Absalom AR, Rodd JM, Johnsrude IS, Matta BF, Owen AM, Menon DK. 2007. Dissociating speech perception and comprehension at reduced levels of awareness. Proc Natl Acad Sci USA. 104:16032-16037.

Demonet JF, Chollet F, Ramsey S. 1993. Language functions explored in normal subjects by positron emission tomography: a critical review. Hum Brain Mapp. 1:39-47.

Demonet JF, Chollet F, Ramsay S, Cardebat D, Nespoulous JL, Wise R, Rascol A, Frackowiak R. 1992. The anatomy of phonological and semantic processing in normal subjects. Brain. 115:1753-1768.

Demonet JF, Price C, Wise R, Frackowiak RS. 1994. Differential activation of right and left posterior sylvian regions by semantic and phonological tasks: a positron-emission tomography study in normal human subjects. Neurosci Lett. 182(1):25-28.

Devlin JT, Matthews PM, Rushworth FS. 2003. Semantic processing in the left prefrontal cortex: a combined functional magnetic resonance imaging and transcranial magnetic stimulation study. J Cogn Neurosci. 15:71-84.

Embick D, Marantz A, Miyashita Y, O'Neil W, Sakai KL. 2000. A syntactic specialisation for Broca's area. Proc Natl Acad Sci USA. 23:6150-6154.

Friederici AD. 2002. Towards a neural basis of auditory sentence processing. Trends Cogn Sci. 6:78-84.

Friederici AD, Meyer M, von Cramon DY. 2000. Auditory language comprehension: an event-related fMRI study on processing of syntax and lexical information. Brain Lang. 74:289-300.

Friederici AD, Ruschemeyer SA, Hahne A, Fiebach CJ. 2003. The role of left inferior frontal and superior temporal cortex in sentence comprehension: localizing syntactic and semantic processes. Cereb Cortex. 13:170-177.

Genovese CR, Lazar NA, Nichols T. 2002. Thresholding of statistical maps in functional neuroimaging using the false discovery rate. Neuroimage. 15:870-878.

Gitelman DR, Nobre AC, Sonty S, Parrish TB, Mesulam MM. 2005. Language network specializations: an analysis with parallel task designs and functional magnetic resonance imaging. Neuroimage. 26(4):975-985.

Glasser MF, Rilling JK. 2008. DTI tractography of the human brain's language pathways. Cereb Cortex. 18(11):2471-2482.

Greicius MD, Supekar K, Menon V, Dougherty RF. 2008. Resting-state functional connectivity reflects structural connectivity in the default mode network. Cereb Cortex. 19(1):72-78.

Gusnard DA, Raichle ME. 2001. Searching for a baseline: functional imaging and the resting human brain. Nat Rev Neurosci. 2:685-694.

Hagoort P. 2005a. Broca's complex as the unification space for language. In: Cutler A, editor. Twenty-first century psycholinguistics: four cornerstones. Mahwah (NJ): Lawrence Erlbaum. p. 157-173.

Hagoort P. 2005b. On Broca, brain, and binding: a new framework. Trends Cogn Sci. 9:416-423.

Hagoort P, Baggio G, Willems RM. Forthcoming. Semantic unification. In: Gazzaniga MS, editor. The new cognitive neurosciences. MIT press.

Hagoort P, Hald L, Bastiaansen M, Petersson KM. 2004. Integration of word meaning and world knowledge in language comprehension. Science. 304:438-441.

Hahne A, Friederici AD. 1999. Electrophysiological evidence for two steps in syntactic analysis: early automatic and late controlled processes. J Cogn Neurosci. 11:194-205.

Hein G, Doehrmann O, Muller NG, Kaiser J, Muckli L, Naumer MJ. 2007. Object familiarity and semantic congruency modulate responses in cortical audiovisual integration areas. J Neurosci. 27:7881-7887.

Hickok G, Poeppel D. 2004. Dorsal and ventral streams: a framework for understanding aspects of the functional anatomy of language. Cognition. 92:67-99.

Hoenig K, Scheef L. 2005. Mediotemporal contributions to semantic processing: fMRI evidence from ambiguity processing during semantic context verification. Hippocampus. 15:597-609.

Horwitz B, Rumsey JM, Donohue BC. 1998. Functional connectivity of the angular gyrus in normal reading and dyslexia. Proc Natl Acad Sci USA. 95:8939-8944.

Indefrey P. 2004. Hirnaktivierungen bei syntaktischer Sprachverarbeitung: eine Meta-Analyse. In: Mueller HM, Rickheit G, editors. Neurokognition der Sprache. Tubingen: Stauffenburg Verlag. p. 31-50.

Indefrey P, Cutler A. 2005. Prelexical and lexical processing in listening. In: Gazzaniga MS, editor. The cognitive neurosciences. Cambridge (MA): MIT Press. p. 759-774.

Jancke L, Wustenberg T, Scheich H, Heinze HJ. 2002. Phonetic perception and the temporal cortex. Neuroimage. 15:733-746.

Jonides J, Schumacher EH, Smith EE, Koeppe RA, Awh E, Reuter-Lorenz PA, Marshuetz C, Willis CR. 1998. The role of parietal cortex in verbal working memory. J Neurosci. 18(13):5026-5034.

Judas M, Cepanec M. 2007. Adult structure and development of the human fronto-opercular cerebral cortex (Broca's region). Clin Linguist Phon. 21(11-12):975-989.

Koechlin E, Ody C, Kouneiher F. 2003. The architecture of cognitive control in the human prefrontal cortex. Science. 302:1181-1185.

Kuperberg GR, Holcomb PJ, Sitnikova T, Greve D, Dale AM, Caplan D. 2003. Distinct patterns of neural modulation during the processing of conceptual and syntactic anomalies. J Cogn Neurosci. 15:272-293.

Kuperberg GR, McGuire PK, Bullmore ET, Brammer MJ, Rabe-Hesketh S, Wright IC, Lythgoe DJ, Williams SC, David AS. 2000. Common and distinct neural substrates for pragmatic semantic and

syntactic processing of spoken sentences: an fMRI study. J Cogn Neurosci. 12:321–341.

Kuperberg GR, Sitnikova T, Lakshmanan BM. 2008. Neuroanatomical distinctions within the semantic system during sentence comprehension: evidence from functional magnetic resonance imaging. Neuroimage. 40:367–388.

Lurito J, Kareken DA, Lowe IJ, Chen SH, Mathews VP. 2000. Comparison of rhyming and word generation with fMRI. Hum Brain Mapp. 10:99–106.

McDermott KB, Petersen SE, Watson JM, Ojemann JG. 2003. A procedure for identifying regions preferentially activated by attention to semantic and phonological relations using functional magnetic resonance imaging. Neuropsychologia. 41:293–303.

Miller EK. 2000. The prefrontal cortex and cognitive control. Nat Rev Neurosci. 1:59–65.

Musso M, Moro A, Glauche V, Rijntjes M, Reichenbach J, Büchel C, Weiller C. 2003. Broca's area and the language instinct. Nat Neurosci. 6:774–781.

Newman AJ, Pancheva R, Ozawa K, Neville HJ, Ullman MT. 2001. An event-related fMRI study of syntactic and semantic violations. J Psycholinguist Res. 30:339–364.

Ni W, Constable RT, Mencl WE, Pugh KR, Fulbright RK, Shaywitz SE, Shaywitz BA, Gore J. 2000. An event-related neuroimaging study distinguishing form and content in sentence processing. J Cogn Neurosci. 12:120–133.

Nishitani N, Schürmann M, Amunts K, Hari R. 2005. Broca's region: from action to language. Physiology. 20:60–69.

Ojemann GA. 1991. Cortical organization of language. J Neurosci. 11: 2281–2287.

Ojemann GA, Mateer C. 1979. Human language cortex: localization of memory, syntax, and sequential motor-phoneme identification systems. Science. 205:1401–1403.

Papanicolaou AC, Pazo-Alvarez P, Castillo EM, Billingsley-Marshall RL, Breier JI, Swank PR, Buchanan S, McManis M, Clear T, Passaro AD. 2006. Functional neuroimaging with MEG: normative language profiles. Neuroimage. 33(1):326–342.

Parker GJ, Luzzi S, Alexander DC, Wheeler-Kingshott CA, Ciccarelli O, Lambon Ralph MA. 2005. Lateralization of ventral and dorsal auditory-language pathways in the human brain. Neuroimage. 24: 656–666.

Paulesu E, Frith CD, Frackowiak RSJ. 1993. The neural correlates of the verbal component of working memory. Nature. 362:342–345.

Poeppel D, Guillemin A, Thompson J, Fritz J, Bavelier D, Braun AR. 2004. Auditory lexical decision, categorical perception, and FM direction discrimination differentially engage left and right auditory cortex. Neuropsychologia. 42:183–200.

Poldrack RA, Wagner AD, Prull MW, Desmond JE, Glover GH, Gabrieli JD. 1999. Functional specialization for semantic and phonological processing in the left inferior prefrontal cortex. Neuroimage. 10:15–35.

Powell HW, Parker GJ, Alexander DC, Symms MR, Boulby PA, Wheeler-Kingshott CA, Barker GJ, Noppeney U, Koepp MJ, Duncan JS. 2006. Hemispheric asymmetries in language-related pathways: a combined functional MRI and tractography study. Neuroimage. 32:388–399.

Price CJ. 1998. The functional anatomy of word comprehension and production. Trends Cogn Sci. 2:281–288.

Price CJ. 2000. The anatomy of language: contributions from functional neuroimaging. J Anat. 197:335–359.

Pugh KR, Mencl WE, Jenner AR, Katz L, Frost SJ, Lee JR, Shaywitz SE, Shaywitz BA. 2001. Neurobiological studies of reading and reading disability. J Commun Disord. 34:479–492.

Rilling JK, Barks SK, Parr LA, Preuss TM, Faber TL, Pagnoni G, Bremner JD, Votaw JR. 2007. A comparison of resting-state brain activity in humans and chimpanzees. Proc Natl Acad Sci USA. 104(43):17146–17151.

Rodd JM, Davis MH, Johnsrude IS. 2005. The neural mechanism of speech comprehension: fMRI studies of semantic ambiguity. Cereb Cortex. 15:1261–1269.

Roelofs A, Hagoort P. 2002. Control of language use: cognitive modeling the hemodynamics of Stroop task performance. Cogn. Brain Res. 15:85–97.

Ruschemeyer SA, Fiebach CJ, Kempe V, Friederici AD. 2005. Processing lexical semantic and syntactic information in first and second language: fMRI evidence from German and Russian. Hum Brain Mapp. 25:266–286.

Sabsevitz DS, Medler DA, Seidenberg M, Binder JR. 2005. Modulation of the semantic system by word imageability. Neuroimage. 27:188–200.

Saffran EM, Marin OS. 1975. Immediate memory for word lists and sentences in a patient with deficient auditory short-term memory. Brain Lang. 24:420–433.

Saffran E, Sholl A. 1999. Clues to the functional and neural architecture of word meaning. In: Brown CM, Hagoort P, editors. The neuro-cognition of language. Oxford: Oxford University Press. p. 241–273.

Sakai KL, Noguchi Y, Takeuchi T, Watanabe E. 2002. Selective priming of syntactic processing by event-related transcranial magnetic stimulation of Broca's area. Neuron. 35:1177–1182.

Scott SK, Johnsrude IS. 2003. The neuroanatomical and functional organization of speech perception. Trends Neurosci. 26:100–107.

Seghier ML, Lazeyras F, Pegna AJ, Annoni JM, Zimine I, Mayer E, Michel CM, Khateb A. 2004. Variability of fMRI activation during a phonological and semantic language task in healthy subjects. Hum Brain Mapp. 23:140–155.

Snijders TM, Vosse T, Kempen G, Van Berkum JJ, Petersson KM, Hagoort P. 2008. Retrieval and unification of syntactic structure in sentence comprehension: an fMRI study using word-category ambiguity. Cereb Cortex. doi: 10.1093/cercor/bhn187.

Stowe LA, Broere CA, Paans AM, Wijers AA, Mulder G, Vaalburg W, Zwarts F. 1998. Localizing components of a complex task: sentence processing and working memory. Neuroreport. 9:2995–2999.

Van Atteveldt N, Formisano E, Goebel R, Blomert L. 2004. Integration of letters and speech sounds in the human brain. Neuron. 43:271–282.

van Heuven WJB, Schriefers H, Dijkstra T, Hagoort P. 2009. Language conflict in the bilingual brain. Cereb Cortex. 18:2706–2716.

Vandenberghe R, Price C, Wise R, Josephs O, Frackowiak RS. 1996. Functional anatomy of a common semantic system for words and pictures. Nature. 383:254–256.

Warrington EK, Shallice T. 1969. The selective impairment of auditory verbal short-term memory. Brain. 92(4):885–896.

Zempleni MZ, Renken R, Hoeks JC, Hoogduin JM, Stowe LA. 2007. Semantic ambiguity processing in sentence context: evidence from event-related fMRI. Neuroimage. 34:1270–1279.